*Proceedings of the 2000 IEEE/RSJ International Conference on Intelligent Robots and Systems*

# Stiffness Analysis for Effective Peg-In/Out-Hole Tasks Using Multi-fingered Robot Hands

Byoung-Ho Kim°,†, Byung-Ju Yi°, Il Hong Suh°, and Sang-Rok Oh†

° : School of Electrical Eng. and Computer Science, Hanyang Univ., Seoul, Korea
† : Intelligent System Control Research Center, KIST, Seoul, Korea
(E-mail: bj@email.hanyang.ac.kr)

**Abstract**

*This paper deals with stiffness analysis for effective peg-in/out-hole tasks using multi-fingered robot hand without inter-finger coupling. We first observe the fact that some of coupling stiffness elements cannot be planned arbitrary. Then, we analyze the conditions of the specified stiffness matrix in the operational space to successfully and more effectively achieve the given peg-in/out-hole tasks. It is concluded that the location of compliance center on the peg and the coupling stiffness element between the translational and the rotational direction play important roles for successful peg-in/out-hole tasks. Simulation results are included to verify the feasibility of the analytic results.*

**Keywords** : *Peg-in/out-hole, Stiffness analysis, Robot hand.*

## 1 Introduction

When an object grasped by a robot hand is being manipulated, explicit force-based fine motion control [1]-[3] may not be practically easy because it is not only hard to implement the force sensor, but also the signal processing of the force signal is not easy. It therefore has been pointed out that instead of explicit force signal the stiffness or compliance is an important quantity for characterizing the grasping and manipulation by robot hands.

Many approaches have been reported in the field of grasp stiffness or compliance [4]-[7]. The stiffness of objects grasped by virtual springs was analyzed in cases of planar and three-dimensional space in [4]. Yokoi, et al. [5] proposed a direct compliance control method and applied the method to a parallel arm. In [6], it is pointed out that a stiffness matrix containing some off-diagonal terms can be useful to prevent jamming of contact tasks. However, the methodology to achieve the desired stiffness characteristic is still an open research field. Recently, Kim, et al. [7] proposed an independent finger/joint-based compliance control method for robot hands manipulating an object, and also the geometric condition for successful implementation of compliance control scheme have been addressed. They showed that an independent finger/joint-based compliance control via redundant actuation was more adequate to modulate the operational stiffness comparing with the case of the kinematically redundant structured fingers or manipulators.

In this paper, an independent finger/joint-based compliance control method is applied to a peg-in/out-hole tasks using robot hands. Related to the peg-in-hole task using robot hands firstly, Whitney [8] classified the geometry of the inserted peg and analyzed the force relations in the peg-in-hole task by using a remote center compliance mechanism. Asada, et al. [9] analyzed the dynamic process of a peg insertion. Matsuoka, et al. [10] used a multi-sensors-based control system to perform a given peg-in-hole task and also proposed a method of executing tasks based on motion primitives for fine manipulation. Shimoga, et al. [11] presented that the desirable location of compliance center should be the point on the grasped object which first touches or which already is in contact with the inserting work piece. An approach to disassembly task was treated in [12]. However, the proper location of compliance center and the determination of stiffness characteristics to effectively achieve the given peg-in-hole task have not been considered yet. Moreover, for the case of peg-out-hole task, there are few research results considering the proper location of compliance center and the determination of stiffness characteristics, where not only peg-in-hole task but also peg-out-hole task is required to consider those factors for suc-

cessful performance practically.

In this paper, we treat both the location of compliance center and the determination of stiffness characteristics for effective peg-in-hole and peg-out-hole tasks. By simulations, it is confirmed that the location of compliance center on the peg and the role of a coupling stiffness element existing between the translational and the rotational direction are important for effective peg-in-hole and peg-out-hole tasks.

## 2 Independent Finger/Joint Based Compliance Control

Consider a rigid peg being inserted in a hole by a three-fingered robot hand in two-dimensional space as shown in Figure 1. The relationship between the

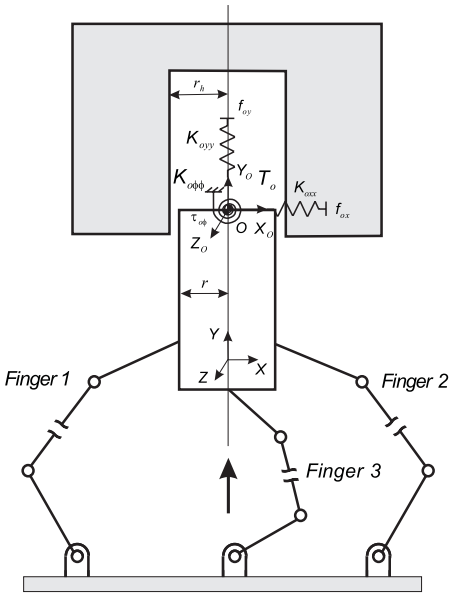


Figure 1: Peg-in-hole task using a three-fingered robot hand.

desired object stiffness matrix $[\boldsymbol{K}_o]$ in the operational space and the stiffness matrix $[\boldsymbol{K}_f]$ in the fingertip space [7] is given as

$$[\boldsymbol{K}_o] = [\boldsymbol{G}_o^f]^T [\boldsymbol{K}_f][\boldsymbol{G}_o^f], \tag{1}$$

where

$$[\boldsymbol{K}_o] = \begin{bmatrix} \boldsymbol{K}_{oxx} & \boldsymbol{K}_{oxy} & \boldsymbol{K}_{ox\phi} \\ \boldsymbol{K}_{oyx} & \boldsymbol{K}_{oyy} & \boldsymbol{K}_{oy\phi} \\ \boldsymbol{K}_{o\phi x} & \boldsymbol{K}_{o\phi y} & \boldsymbol{K}_{o\phi\phi} \end{bmatrix},$$

and $[\boldsymbol{G}_o^f]$ denotes the Jacobian relating the fingertip space to the task space.

In [7], it is analyzed that a robot hand should have at least three fingers to modulate $3 \times 3$ object stiffness characteristic in two-dimensional space. An alternative form of (1) can be expressed by

$$K_{oo} = [\boldsymbol{B}_f^o]\, K_{ff}, \tag{2}$$

where

$$K_{oo} = [\boldsymbol{K}_{oxx}\ \boldsymbol{K}_{oxy}\ \boldsymbol{K}_{ox\phi}\ \boldsymbol{K}_{oyy}\ \boldsymbol{K}_{oy\phi}\ \boldsymbol{K}_{o\phi\phi}]^T,$$

$$[\boldsymbol{B}_f^o] = \begin{bmatrix} 1.0 & 0.0 & 1.0 & 0.0 & 1.0 & 0.0 \\ 0.0 & 0.0 & 0.0 & 0.0 & 0.0 & 0.0 \\ y_1 & 0.0 & y_2 & 0.0 & y_3 & 0.0 \\ 0.0 & 1.0 & 0.0 & 1.0 & 0.0 & 1.0 \\ 0.0 & -x_1 & 0.0 & x_2 & 0.0 & x_3 \\ y_1^2 & x_1^2 & y_2^2 & x_2^2 & y_3^2 & x_3^2 \end{bmatrix},$$

$$K_{ff} = [{}^1\boldsymbol{K}_{fxx}\ {}^1\boldsymbol{K}_{fyy}\ {}^2\boldsymbol{K}_{fxx}\ {}^2\boldsymbol{K}_{fyy}\ {}^3\boldsymbol{K}_{fxx}\ {}^3\boldsymbol{K}_{fyy}]^T,$$

and $y_i$, $x_i$ denote the elements of position vectors directing from the $i$th finger contact position to the task position, and they are given all positive. $[{}^i\boldsymbol{K}_{fxx}]$ and $[{}^i\boldsymbol{K}_{fyy}]$ represent the $x$- and $y$-directional stiffness elements in the fingertip space of the $i$th finger, respectively.

Note that the elements of the second row of the mapping matrix $[\boldsymbol{B}_f^o]$ in (2) are calculated as zero. This is because we excluded the coupling terms ${}^i\boldsymbol{K}_{fxy}(i{=}1,\ 2,\ 3)$ in the fingertip space for independent compliance control. Thus, we have zero $\boldsymbol{K}_{oxy}$, which, in fact, is a linear combination of ${}^i\boldsymbol{K}_{fxy}(i{=}1, 2, 3)$. Also, note that the third row of $[\boldsymbol{B}_f^o]$ corresponds to modulation of $\boldsymbol{K}_{ox\phi}$. However, we can easily notice that zero $\boldsymbol{K}_{ox\phi}$ cannot be achieved by all positive stiffness components $K_{ff}$ defined in the fingertip space since the three influence coefficients (i.e., $y_1$, $y_2$, and $y_3$) are always positive in this grasped configuration.

Consider a modified posture of grasp in Figure 2, in which the contact position of the third finger lies above the task position $\boldsymbol{O}$. In this case, the (3, 5) element of $[\boldsymbol{B}_f^o]$ is converted to $-y_3$ and thus, zero $\boldsymbol{K}_{ox\phi}$ can be achieved. However, since the posture of grasp as shown in Figure 2 is not allowed in a peg-in-hole task, zero $\boldsymbol{K}_{ox\phi}$ cannot be obtained. Therefore, $\boldsymbol{K}_{ox\phi}$ always exists.

Let $[\boldsymbol{D}_f^o]$ be the matrix excluding the second and third rows of $[\boldsymbol{B}_f^o]$ and $K_{oo}^*$ be the vector excluding $\boldsymbol{K}_{oxy}$ and $\boldsymbol{K}_{ox\phi}$ of $K_{oo}$. Then, $K_{ff}^*$ can be obtained as follows:

$$K_{ff}^* = [\boldsymbol{D}_f^o]^+ K_{oo}^*. \tag{3}$$

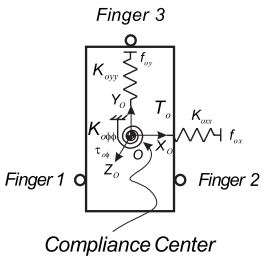


Figure 2: A three-fingered grasp.

Next, the coupling stiffness element $\boldsymbol{K}_{ox\phi}$ can be determined by

$$\boldsymbol{K}_{ox\phi} = [\boldsymbol{B}_f^o]_3 \; K_{ff}^*, \tag{4}$$

where $[\boldsymbol{B}_f^o]_3$ denotes the third row of $[\boldsymbol{B}_f^o]$.

## 3 Analysis of Compliance Characteristic for Assembling Task

In the paper, we consider the peg-in/out-hole problems, respectively, in a quasi-static state.

### 3.1 Peg-In-Hole Task

When a rigid peg being inserted in a hole by three-fingered robot hand in two-dimensional space, let us consider that a left-side of the peg is being contacted on the hole as shown in Figure 3 by $x$-directional position error and hence the peg is taken some $x$-directional reaction force.

The forces exerted on the virtual springs attached to the peg tip can be expressed as

$$\begin{bmatrix} f_{ox} \\ f_{oy} \\ \tau_{o\phi} \end{bmatrix} = \begin{bmatrix} \boldsymbol{K}_{oxx} & 0 & \boldsymbol{K}_{ox\phi} \\ 0 & \boldsymbol{K}_{oyy} & 0 \\ \boldsymbol{K}_{o\phi x} & 0 & \boldsymbol{K}_{o\phi\phi} \end{bmatrix} \begin{bmatrix} \delta u_{ox} \\ \delta u_{oy} \\ \delta u_{o\phi} \end{bmatrix}, \tag{5}$$

where the small deflections of the virtual springs in the $x$-, $y$-, and rotational directions, respectively, are given by

$$\begin{aligned} \delta u_{ox} &= u_{ox}^d - u_{ox}^a, \\ \delta u_{oy} &= u_{oy}^d - u_{oy}^a, \\ \delta u_{o\phi} &= u_{o\phi}^d - u_{o\phi}^a, \end{aligned}$$

and here $u_{oj}^d$ and $u_{oj}^a$ denote the $j$-directional desired and actual position, respectively.

The $x$-directional force $f_{ox}$, $y$-directional force $f_{oy}$, and torque $\tau_{o\phi}$, which are induced by the $x$-directional reaction force($f_{rox} > 0$), are given by

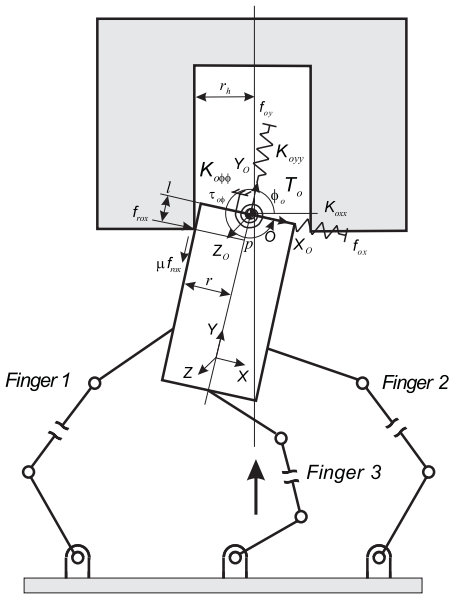


Figure 3: Left-side contact

$$f_{ox} = -f_{rox}, \tag{6}$$

$$f_{oy} = -\mu f_{rox}, \tag{7}$$

$$\tau_{o\phi} = f_{rox}(l + \mu r), \tag{8}$$

where $\mu$, $l$, and $r$ denote the friction coefficient at the contacting surface, the length between the compliance center and the point $p$, and the radius of peg, respectively.

If a virtual desired path to be followed is intentionally given to be inside the surface of the hole, the small deflection $\delta u_{ox}$ of the virtual spring in the $x$-direction becomes negative. Thus, a positive directional reaction force and its associated friction force are generated, and simultaneously, the orientation change of the peg is occurred by the torque caused by the reaction forces. From equations (5), (6), and (8), the torque relation at the compliance center can be given by

$$\begin{aligned} &\boldsymbol{K}_{ox\phi}\delta u_{ox} + \boldsymbol{K}_{o\phi\phi}\delta u_{o\phi} = \\ &\quad -\boldsymbol{K}_{oxx}(l + \mu r)\delta u_{ox} - \boldsymbol{K}_{ox\phi}(l + \mu r)\delta u_{o\phi}. \end{aligned} \tag{9}$$

By rearranging (9), we have

$$\delta u_{o\phi} = -\left\{ \frac{\boldsymbol{K}_{ox\phi} + \boldsymbol{K}_{oxx}(l + \mu r)}{\boldsymbol{K}_{o\phi\phi} + \boldsymbol{K}_{ox\phi}(l + \mu r)} \right\} \delta u_{ox}. \tag{10}$$

Note that since the sign of the value inside parenthesis is always given positive and $\delta u_{ox}$ is negative in this case, the orientation change by touching the left-side of the peg on the hole is at least greater than

zero from (10) and hence the inserted peg rotate to the counterclockwise direction about the compliance center. Therefore, this phenomena facilitates the insertion task. Even though $l$=0 and $\mu$=0, existence of $\boldsymbol{K}_{ox\phi}$ makes the insertion job successful.

Then, consider the case that a right-side of the peg is being contacted on the hole as shown in Figure 4.

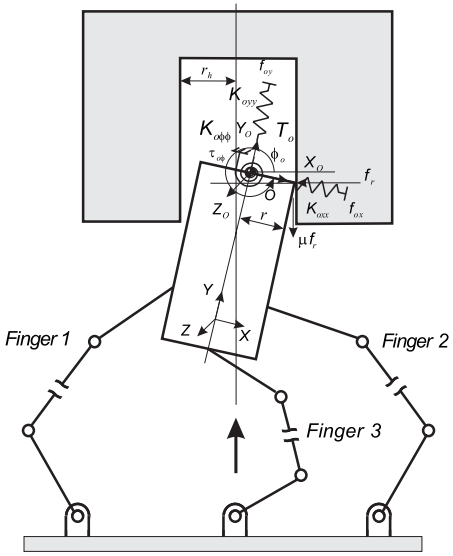


Figure 4: Right-side contact

The forces exerted on the virtual springs of attached to the peg are derived as

$$f_{ox} = f_r \{cos(\phi_o) + \mu sin(\phi_o)\}, \quad (11)$$

$$f_{oy} = -f_r \{sin(\phi_o) + \mu cos(\phi_o)\}, \quad (12)$$

$$\tau_{o\phi} = -r f_{ox} \sigma, \quad (13)$$

where

$$\sigma = -\left\{\frac{tan(\phi_o) - \mu}{1 + \mu tan(\phi_o)}\right\} \geq 0, \quad \phi_{o,min} \leq \phi_o \leq 2\pi,$$

$$\phi_{o,min} = \frac{3\pi}{2} + cos^{-1}\left(\frac{r}{r_h}\right),$$

$\phi_{o,min}$ and $r_h$ denote the minimum orientation angle of the peg and the radius of the hole, respectively.

When a right-side of the peg is being contacted on the hole, some negative directional reaction forces and its associated friction force are generated, and simultaneously, the orientation change of the peg is occurred by the torque caused by the reaction forces. From equations (5), (11), and (13), the torque relation at the compliance center can be given by

$$\boldsymbol{K}_{ox\phi}\delta u_{ox} + \boldsymbol{K}_{o\phi\phi}\delta u_{o\phi} = -r\boldsymbol{K}_{oxx}\sigma\delta u_{ox} - r\boldsymbol{K}_{ox\phi}\sigma\delta u_{o\phi}. \quad (14)$$

By rearranging (14), we have

$$\delta u_{o\phi} = -\left\{\frac{\boldsymbol{K}_{ox\phi} + r\boldsymbol{K}_{oxx}\sigma}{\boldsymbol{K}_{o\phi\phi} + r\boldsymbol{K}_{ox\phi}\sigma}\right\}\delta u_{ox}. \quad (15)$$

From (15), note that the sign of the value inside parentheses is always positive. Since $\delta u_{ox}$ is always taken positive in this contact type, $\delta u_{o\phi}$ becomes negative. This results clockwise rotation of the peg, which is undesirable for peg insertion.

Now, consider the peg-in-hole task shown in Figure 5, where the location of compliance center is modified. In Figure 5, the length parameters, $c$ and $a$, and $\alpha$

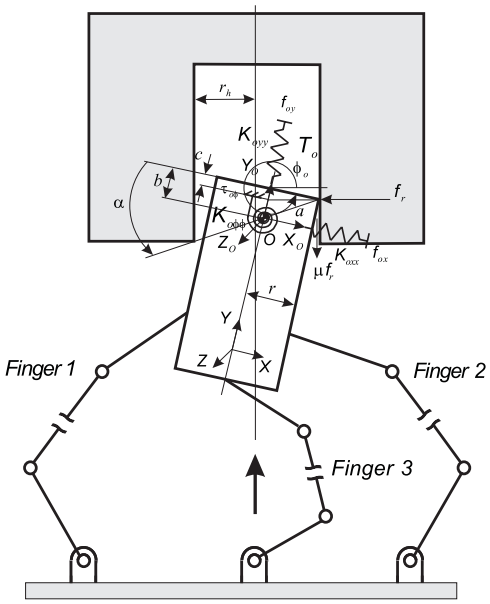


Figure 5: Modified right-side contact.

angle are computed as

$$c = r|tan(\phi_o)|, \quad (16)$$

$$a = \sqrt{r^2 + b^2}, \quad (17)$$

$$\alpha = cos^{-1}\left(\frac{r}{a}\right), \quad (18)$$

where $b$ is the distance from the peg tip to the compliance center and it is a design parameter to be determined.

When we set $b$ larger than $c$, the $x$- and $y$-directional forces, and torque induced by the $x$-directional reaction force($f_r > 0$) are given by

$$f_{ox} = f_r \{cos(\phi_o) + \mu sin(\phi_o)\}, \quad (19)$$

$$f_{oy} = -f_r \{sin(\phi_o) + \mu cos(\phi_o)\}, \quad (20)$$

$$\tau_{o\phi} = a f_{ox} \lambda, \quad (21)$$

where $\lambda$ is defined as

$$\lambda = \frac{sin(\alpha) + cos(\alpha)tan(\phi_o) - \mu\{cos(\alpha) - sin(\alpha)tan(\phi_o)\}}{1 + \mu tan(\phi_o)}$$

and here, if the $\alpha$ angle is properly determined by setting the distance $b$, the sign of $\lambda$ can be set up to be positive in most case.

From equations ( 5), (19), and (21), the torque relation at the compliance center can be given by

$$\boldsymbol{K}_{ox\phi}\delta u_{ox} + \boldsymbol{K}_{o\phi\phi}\delta u_{o\phi} = a\boldsymbol{K}_{oxx}\lambda\delta u_{ox} + a\boldsymbol{K}_{ox\phi}\lambda\delta u_{o\phi}. \quad (22)$$

By rearranging (22), the orientation change of the peg can be expressed as

$$\delta u_{o\phi} = -\left\{\frac{\boldsymbol{K}_{ox\phi} - a\boldsymbol{K}_{oxx}\lambda}{\boldsymbol{K}_{o\phi\phi} - a\boldsymbol{K}_{ox\phi}\lambda}\right\}\delta u_{ox}. \quad (23)$$

In this case, the orientation change of the peg is at least greater than zero if either of the following conditions are satisfied.

$$\delta u_{o\phi} = -\left\{\frac{\boldsymbol{K}_{ox\phi} - a\boldsymbol{K}_{oxx}\lambda}{\boldsymbol{K}_{o\phi\phi} - a\boldsymbol{K}_{ox\phi}\lambda}\right\}\delta u_{ox}, \quad \boldsymbol{K}_{ox\phi} > a\boldsymbol{K}_{oxx}\lambda \text{ and } \boldsymbol{K}_{o\phi\phi} < a\boldsymbol{K}_{ox\phi}\lambda, \quad (24)$$

$$\delta u_{o\phi} = -\left\{\frac{\boldsymbol{K}_{ox\phi} - a\boldsymbol{K}_{oxx}\lambda}{\boldsymbol{K}_{o\phi\phi} - a\boldsymbol{K}_{ox\phi}\lambda}\right\}\delta u_{ox}, \quad \boldsymbol{K}_{ox\phi} < a\boldsymbol{K}_{oxx}\lambda \text{ and } \boldsymbol{K}_{o\phi\phi} > a\boldsymbol{K}_{ox\phi}\lambda. \quad (25)$$

From equations (24) and (25), we can notice that the stiffness elements in the operational space should be carefully selected for effective handling of the given peg-in-hole task.

### 3.2 Peg-Out-Hole Task

Consider the task of disassembling peg from a hole, as shown in Figure 6, where the peg contacts the left-side of the hole.

When the location of compliance center lies in the origin denoted $\boldsymbol{O}_1$, $\boldsymbol{O}_2$, $\boldsymbol{O}_3$, and $\boldsymbol{O}_4$ in Figure 6, respectively, the orientation change of the peg for each case can be described as, respectively,

$$\delta u_{o\phi} = -\left\{\frac{\boldsymbol{K}_{ox\phi} + \boldsymbol{K}_{oxx}(l_1 - \mu r)}{\boldsymbol{K}_{o\phi\phi} + \boldsymbol{K}_{ox\phi}(l_1 - \mu r)}\right\}\delta u_{ox}, \quad (26)$$

$$\delta u_{o\phi} = -\left\{\frac{\boldsymbol{K}_{ox\phi} + \boldsymbol{K}_{oxx}(l_2 - \mu r)}{\boldsymbol{K}_{o\phi\phi} + \boldsymbol{K}_{ox\phi}(l_2 - \mu r)}\right\}\delta u_{ox}, \quad (27)$$

$$\delta u_{o\phi} = -\left\{\frac{\boldsymbol{K}_{ox\phi} - \boldsymbol{K}_{oxx}(l_3 + \mu r)}{\boldsymbol{K}_{o\phi\phi} - \boldsymbol{K}_{ox\phi}(l_3 + \mu r)}\right\}\delta u_{ox}, \quad (28)$$

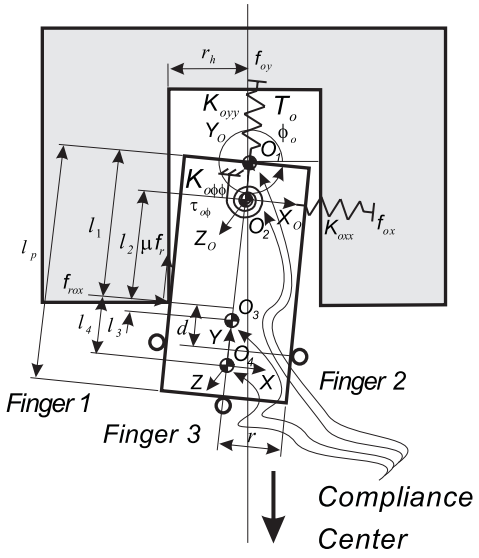


Figure 6: Peg-out-hole: left-side contact.

and

$$\delta u_{o\phi} = -\left\{-\frac{\boldsymbol{K}_{oxx}(l_4 + \mu r)}{\boldsymbol{K}_{o\phi\phi}}\right\}\delta u_{ox}, \quad (29)$$

where $l_i (i = 1, \cdots, 4)$ denotes the distance between the contact point and the location of the $i$th compliance center, respectively. Particularly, if the compliance center moves from $\boldsymbol{O}_3$ to $\boldsymbol{O}_4$, $\boldsymbol{K}_{ox\phi}$ in (28) can be specified zero by the independent finger-based compliance control method proposed in [7]. Thus, the orientation change $\delta u_{o\phi}$ of the peg can be expressed by (29) and also its sign has always negative since $\delta u_{ox}$ is given negative(as discussed in section 3.1).

Note that $l_i (i = 1, \cdots, 4)$, and $r$ are given very small and also $\mu$ is small. Thus, the signs of the value inside parentheses in (26) and (27) are positive, while those of the value inside parentheses in (28) and (29) are negative in most cases. Since $\delta u_{ox}$ is taken negative always, $\delta u_{o\phi}$ in (26) and (27) becomes positive, and hence the peg rotate to the counterclockwise direction about the compliance center in those cases. Also, $\delta u_{o\phi}$ becomes larger as the location of the compliance center is located near the peg tip. On the contrary, $\delta u_{o\phi}$ in (28) and (29) becomes negative, resulting in clockwise rotation of the peg which is undesirable for this task. This observation seems to be somewhat surprising, since compliance center for disassembly task of peg-in-hole has been usually believed to be chosen as $\boldsymbol{O}_3$ or $\boldsymbol{O}_4$. Thus, it is necessary to properly plan the location of the compliance center, in on-line fashion, for effective disassembly task.

Next, consider the case when the peg contacts the right-side of the hole.

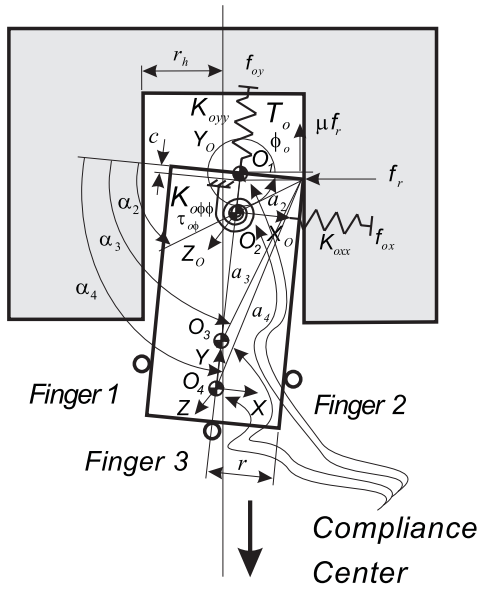


Figure 7: Peg-out-hole: right-side contact.

When the location of compliance center lies in the origin denoted $\boldsymbol{O}_1$ in Figure 7, the orientation change of the peg can be represented by

$$\delta u_{o\phi} = -\left\{\frac{\boldsymbol{K}_{ox\phi} - r\boldsymbol{K}_{oxx}\rho}{\boldsymbol{K}_{o\phi\phi} - r\boldsymbol{K}_{ox\phi}\rho}\right\}\delta u_{ox}, \tag{30}$$

where a variable $\rho$ is defined as

$$\rho = \frac{\mu + tan(\phi_o)}{1 - \mu tan(\phi_o)} \geq 0, \quad \text{for} \quad \mu \geq |tan(\phi_o)|.$$

Also, we can obtain the orientation change of the peg as the location of compliance center moves to $\boldsymbol{O}_2$ and $\boldsymbol{O}_3$ as follows:

$$\delta u_{o\phi} = -\left\{\frac{\boldsymbol{K}_{ox\phi} - a_i\boldsymbol{K}_{oxx}\eta_i}{\boldsymbol{K}_{o\phi\phi} - a_i\boldsymbol{K}_{ox\phi}\eta_i}\right\}\delta u_{ox}, \tag{31}$$

where $a_i (i = 2, 3)$ denotes the distance between the contact point and the $i$th compliance center and the positive variable $\eta_i (i = 2, 3)$ for the $i$th compliance center is defined as

$$\eta_i = \left\{\frac{sin(\alpha_i) + cos(\alpha_i)tan(\phi_o)}{1 - \mu tan(\phi_o)}\right\} + \left\{\frac{\mu\{cos(\alpha_i) - sin(\alpha_i)tan(\phi_o)\}}{1 - \mu tan(\phi_o)}\right\}. \tag{32}$$

Particularly, if the location of compliance center lies in the origin $\boldsymbol{O}_4$, $\boldsymbol{K}_{ox\phi}$ can be specified zero by the independent finger-based compliance control method proposed in [7], and therefore we have always positive $\delta u_{o\phi}$ as follows:

$$\delta u_{o\phi} = \left\{\frac{a_4\boldsymbol{K}_{oxx}\eta_4}{\boldsymbol{K}_{o\phi\phi}}\right\}\delta u_{ox}, \tag{33}$$

where $\eta_4$ is determined by (32).

Since $\delta u_{ox}$ is given positive, from (30), (31), and (33), we can notice that if the distance between the peg tip and the compliance center is greater or equal to $c$, $\delta u_{o\phi}$ can be made positive with proper selection of stiffness elements.

In other way, if the peg rotates too much before the peg comes out from the hole, the peg comes to have a similar posture as Figure 6, where the left-side contacts the hole. In this case, the mode of stiffness planning should be changed so that the peg should have its desired rotational motion. Otherwise, the motion planning of the peg is such that the peg leave the hole before the other edge of the peg contact the wall.

Now, we can provide a guideline for selecting the location of compliance center for effective peg-in/out-hole task in Table 1.

Table 1. Effective location of compliance center.

| Task | LCC | Left | Right | Range of LCC |
|---|---|---|---|---|
| PIH | $\boldsymbol{O}_1$ | ◯ | X | $0 \leq l_c < c$ |
| | $\boldsymbol{O}_2$ | ◯ | △ | $c \leq l_c \leq l_1$ |
| | $\boldsymbol{O}_3$ | X | △ | $l_1 < l_c \leq l_1 + d$ |
| | $\boldsymbol{O}_4$ | X | ◯ | $l_1 + d < l_c < l_p$ |
| POH | $\boldsymbol{O}_1$ | △ | X | $0 \leq l_c < c$ |
| | $\boldsymbol{O}_2$ | △ | △ | $c \leq l_c \leq l_1$ |
| | $\boldsymbol{O}_3$ | X | △ | $l_1 < l_c \leq l_1 + d$ |
| | $\boldsymbol{O}_4$ | X | ◯ | $l_1 + d < l_c < l_p$ |

PIH, POH, and LCC in Table 1 denote the abbreviation of peg-in-hole, peg-out-hole, and the location of compliance center, respectively, and $l_c$ is the distance between the peg tip and the compliance center. And ◯, △, and X mean effective, conditionally effective, and not desired status for the given task, respectively.

From Table 1, since the effectiveness to the given tasks differ as the location of compliance center, we can conclude that the location of compliance center on the peg should be properly planned for more effective peg-in/out-hole tasks and also, the range of the compliance center denoted $\boldsymbol{O}_2$ may be suitable for conditionally stable task by planning the stiffness characteristics in the operational space.

A similar analysis can be possibly performed for the case that both the left- and right-sides of peg simultaneously contact on the hole.

## 4 Simulation Results

This section provides simulation results to confirm the orientation change of the peg when the peg contacts the hole. In simulations, we use a three-fingered robot hand equipped with five bar mechanism [7, 13]. The desired stiffness matrix in the operational space is specified as

$$\boldsymbol{K}_o = \begin{bmatrix} \boldsymbol{K}_{oxx} & \boldsymbol{K}_{oxy} & \boldsymbol{K}_{ox\phi} \\ \boldsymbol{K}_{oyx} & \boldsymbol{K}_{oyy} & \boldsymbol{K}_{oy\phi} \\ \boldsymbol{K}_{o\phi x} & \boldsymbol{K}_{o\phi y} & \boldsymbol{K}_{o\phi\phi} \end{bmatrix} = \begin{bmatrix} 100 & 0 & 1.37 \\ 0 & 1500 & 0 \\ 1.37 & 0 & 0.5 \end{bmatrix}, \quad (34)$$

where $\boldsymbol{K}_{ox\phi}$ is determined by (4).

The grasp points of the three-fingered robot hand are given $(-x_1, -y_1) = (-0.03, -0.06)$, $(x_2, -y_2) = (0.03, -0.06)$, and $(x_3, -y_3) = (0.0, -0.1)$, where sign of all parameters are set positive and those unit is meter. The material of the peg and the hole is assumed wood. The friction coefficient $\mu$ and the initial orientation of the peg are set as 0.3 and $350^o$, respectively.

The first simulation corresponds to Figure 3, where the parameter $l$ is fixed as $0.03m$. The second simulation considers the case of Figure 4. the third simulation treats the same task with modified compliance center as shown in Figure 5, where the distance parameter $b$ is set as $0.05m$. Finally, simulations for the peg-out-hole task are performed.

Simulation results for the peg-in-hole task are shown in Figures 8, 9, and 10, respectively. Figures 8 shows that the orientation of the inserted peg changes properly upon contacting the left-side of the peg on the hole. Note that the orientation of the peg in the case (a) of Figure 9 decrease for the $x$-directional deflection, while that of the peg in the case (b) of Figure 9 increase. Consequently, it can be said that the given peg-in-hole task is more easily achieved in the case (b) comparing to the case (a). From Figure 10, it is confirmed that the necessary conditions described in the equation (25) are satisfied during the contact.

Simulation results for the peg-out-hole task are shown in Figures 11 and 12, where the length parameters(unit: $m$) $l_1, l_2, l_3, l_4, l_p$, and $d$ are set as 0.04, 0.01, 0.01, 0.035, 0.1, and 0.02, respectively. Figure 11 shows that when the location of compliance center locates in either $\boldsymbol{O}_1$ or $\boldsymbol{O}_2$, the orientation of the peg increases for the $x$-directional deflection, while that of the peg in either $\boldsymbol{O}_3$ or $\boldsymbol{O}_4$ decreases. Figure 12 shows the orientation of the peg for right-side contact. We can see the orientation of the peg increases for all cases except $\boldsymbol{O}_1$.

It is observed the orientation of the peg may decrease always or conditionally when a compliance center on the peg is located in $\boldsymbol{O}_1$, $\boldsymbol{O}_3$, and $\boldsymbol{O}_4$. Thus, the compliance center $\boldsymbol{O}_2$ is best for effective peg-in/out-hole tasks. Also, we can confirm that planning the location of the compliance center on the peg is necessary for effective peg-in/out-hole tasks. From the above analysis, it is concluded that the location of compliance center on the peg should be properly chosen for effective peg-in/out-hole tasks and also the coupling stiffness element existing between the $x$-direction and the rotational direction plays important roles in peg-in/out-hole tasks.

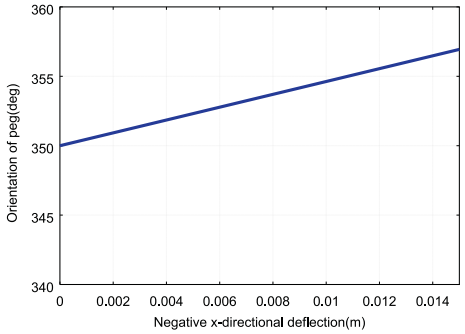


Figure 8: Orientation of the peg for left-side contact.

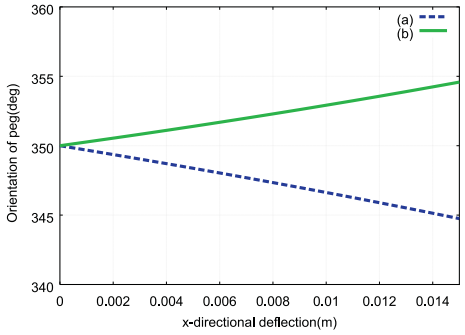


Figure 9: Orientation of the peg for right-side contact: (a) is the case that the compliance center lies in the peg tip and (b) is the case that the location of compliance center is modified.

## 5 Concluding Remarks

In this paper, we analyzed the conditions of the specified stiffness matrix in the operational space to

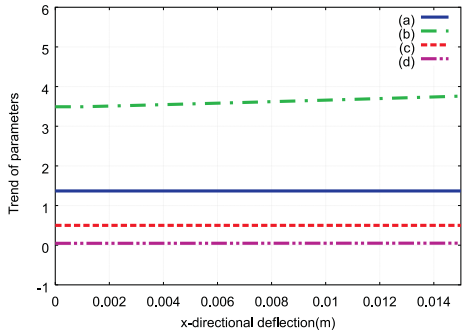


Figure 10: Trend of parameters: (a) $\boldsymbol{K}_{ox\phi}$ (b) $a\boldsymbol{K}_{oxx}\lambda$ (c) $\boldsymbol{K}_{o\phi\phi}$ (d) $a\boldsymbol{K}_{ox\phi}\lambda$.

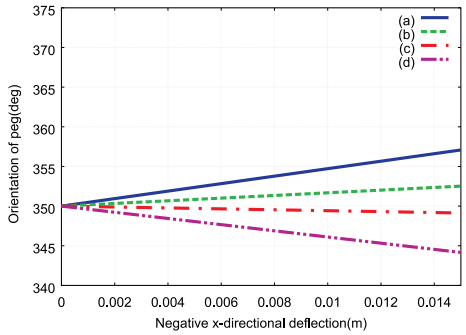


Figure 11: Orientation of the peg for left-side contact in the peg-out-hole task: (a) $\boldsymbol{O}_1$ (b) $\boldsymbol{O}_2$ (c) $\boldsymbol{O}_3$ (d) $\boldsymbol{O}_4$.

successfully and more effectively achieve the defined peg-in/out-hole tasks including analysis of efficiency for the tasks as the location of compliance center. Through the analysis, it is concluded that the location of compliance center on the peg and the coupling stiffness element existing between the translational and the rotational direction play important roles for successful insertion and disassembly tasks.

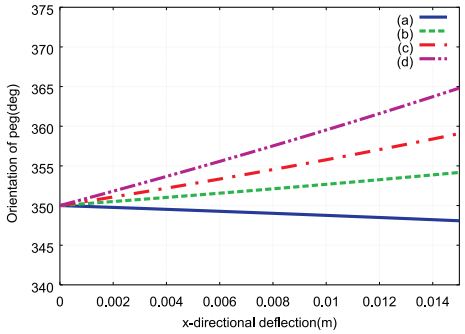


Figure 12: Orientation of the peg for right-side contact in the peg-out-hole task: (a) $\boldsymbol{O}_1$ (b) $\boldsymbol{O}_2$ (c) $\boldsymbol{O}_3$ (d) $\boldsymbol{O}_4$.

## References


[1] T. Yoshikawa, and X. -Z. Zheng, "Coordinated dynamic hybrid position/force control for multiple robot manipulators handling one constrained object," *Int. Jour. of Robotics Research*, Vol. 12, No. 3, pp. 219-230, 1993.

[2] T. Hasegawa, T. Matsuoka, T. Kiriki, and K, Honda, "Manipulation of an object by a multi-fingered hand with multi-sensors," *Proc. of Int. Conf. on Industrial Electronics, Control, and Instrumentation*, pp. 174-179, 1996.

[3] H. Maekawa, K. Tanie, and K. Komoria, "Dynamic Grasping Force Control Using Tactile Feedback for Grasp of Multifingered Hand," *Proc. of IEEE Int. Conf. on Robotics and Automation*, pp. 2462-2469, April 1996.

[4] V. Nguyen, "Constructing Force-Closure Grasps in 3-D," *Proc. of IEEE Int. Conf. on Robotics and Automation*, pp. 240-245, March 1987.

[5] K. Yokoi, M. Kaneko, and K. Tanie, "A Compliance Control Method Suggested by Muscle Networks In Human Arms," *Proc. of IEEE/RSJ Int. Conf. on Intelligent Robots and Systems*, pp. 385-390, 1988.

[6] M. H. Ang, Jr. and G. B. Andeen, "Specifying and Achieving Passive Compliance Based on Manipulator Structure," *IEEE Trans. on Robotics and Automation*, Vol. 11, No. 4, pp. 504-515, 1995.

[7] B. -H. Kim, B. -J. Yi, I. H. Suh, and S. -R. Oh, "A Biomimetic Compliance Control of Robot Hand by Considering Structures of Human Finger," *Proc. of IEEE Int. Conf. on Robotics and Automation*, April 2000.

[8] D. E. Whitney, "Quasi-Static Assembly of Compliantly Supported Rigid Parts," *Jour. of Dynamic systems, Measurement, and control*, Vol. 104, pp. 65-77, March 1982.

[9] H. Asada, Y. Kakumoto, "The Dynamic Analysis and Design of a High-Speed Insertion Hand Using the Generalized Centroid and Virtual Mass," *Jour. of Dynamic systems, Measurement, and control*, Vol. 112, pp. 646-652, 1990.

[10] T. Matsuoka, T. Hasegawa, T. Kiriki, and K, Honda, "Mechanical Assembly based on Motion Primitives of Multi-fingered Hand," *Proc. of Advanced Intelligent Mechatronics*, 1997.

[11] K. B. Shimoga and A. A. Goldenberg, "Grasp Admittance Center: Choosing Admittance Center Parameters," *Proc. of American Control Conference*, pp. 2527-2532, 1991.

[12] P. Dario and M. Rucci, "An Approach to Disassembly Problems in Robotics," *Proc. of IEEE/RSJ Int. Conf. on Intelligent Robots and Systems*, pp. 460-467, 1993.

[13] B. -J. Yi, I. H. Suh, and S. -R. Oh, "Analysis of a five-bar finger mechanism having redundant actuators with applications to stiffness and frequency modulation," *Proc. of IEEE Int. Conf. on Robotics and Automation*, pp. 759-765, 1997.